

# Phase diagram for non-axisymmetric plasma balls

Vitor Cardoso,<sup>1,2</sup> Óscar J. C. Dias,<sup>3</sup> Jorge V. Rocha,<sup>1</sup>

<sup>1</sup> *CENTRA, Dept. de Física, Instituto Superior Técnico,  
Av. Rovisco Pais 1, 1049-001 Lisboa, Portugal*

<sup>2</sup> *Dept. of Physics and Astronomy, The University of Mississippi,  
University, MS 38677-1848, USA*

<sup>3</sup> *DAMTP, Centre for Mathematical Sciences, University of Cambridge,  
Wilberforce Road, Cambridge CB3 0WA, United Kingdom*

vitor.cardoso@ist.utl.pt, O.Dias@damtp.cam.ac.uk, jorge.v.rocha@ist.utl.pt

## ABSTRACT

Plasma balls and rings emerge as fluid holographic duals of black holes and black rings in the hydrodynamic/gravity correspondence for the Scherk-Schwarz AdS system. Recently, plasma balls spinning above a critical rotation were found to be unstable against  $m$ -lobed perturbations. In the phase diagram of stationary solutions the threshold of the instability signals a bifurcation to a new phase of non-axisymmetric configurations. We find explicitly this family of solutions and represent them in the phase diagram. We discuss the implications of our results for the gravitational system. Rotating non-axisymmetric black holes necessarily radiate gravitational waves. We thus emphasize that it would be important, albeit possibly out of present reach, to have a better understanding of the hydrodynamic description of gravitational waves and of the gravitational interaction between two bodies. We also argue that it might well be that a non-axisymmetric  $m$ -lobed instability is also present in Myers-Perry black holes for rotations below the recently found ultraspinning instability.

# Contents

<b>1</b>	<b>Introduction</b>	<b>1</b>
<b>2</b>	<b>Hydrodynamics of stationary plasma lumps</b>	<b>3</b>
2.1	Relativistic hydrodynamic equations . . . . .	3
2.2	Stationary plasmas . . . . .	4
2.3	Conserved charges . . . . .	5
<b>3</b>	<b>Stationary solutions: balls, rings and lobed plasmas</b>	<b>6</b>
3.1	Axisymmetric solutions: plasma balls and plasma rings . . . . .	6
3.2	Plasma peanuts and $m$ -lobed configurations . . . . .	7
3.2.1	Boundary equation for lobed plasmas . . . . .	7
3.2.2	Lobed plasmas from perturbed analysis of plasma balls . . . . .	9
3.2.3	Phase diagram of stationary plasmas . . . . .	11
3.3	No $m$ -lobed plasma rings . . . . .	12
3.4	The hydrodynamic regime . . . . .	14
<b>4</b>	<b>Gravity duals. Discussion</b>	<b>14</b>
<b>A</b>	<b>Non-relativistic lobed configurations</b>	<b>17</b>

## 1 Introduction

The idea of an hypothetical connection between black holes and fluid balls has been the subject of several studies along the decades. Nevertheless, for a long time no formal map between these two distinct systems was available. (Although the membrane paradigm, whereby a black hole horizon is mimicked by a stretched fluid membrane, provided an interesting analogue model with useful applications in astrophysical systems). However, the state of the art changed radically in recent years. Motivated by the AdS/CFT duality and by Landau’s observation that any quantum field theory should have an effective hydrodynamic description at high energy densities (where the mean free path of the theory is small), a rigorous duality between gravity and hydrodynamics was finally found. Emerging with the path-breaking studies [1, 2], themselves motivated by the ideas of [3]–[8], this duality has been since then successfully explored in a series of works [9]–[29]; for a nice review and references see [30].

The main idea is as follows [1, 2, 30]. Start with a black hole solution of Einstein-AdS gravity and divide its horizon in several patches. Consider then the approximation where in the tubewise region that goes from each horizon patch up to the AdS boundary the geometry is approximately described by the line element of a boosted planar black brane. This is parametrized by the temperature  $T$  and boost parameters  $\beta_i$  along the timelike and boundary spacelike coordinates  $x^i$ . When moving along the several patches one allows the temperature and boosts to vary slowly with the boundary coordinates. Obviously such a patched geometry will generically not be a solution of Einstein-AdS

gravity. However, it will be a solution at any order of a perturbative expansion of the Einstein-AdS field equations as long as at each order  $n$  the holographic stress tensor  $T_{(n)}^{\mu\nu}$  satisfies certain equations that turn out to be simply  $\nabla_\nu T_{(n)}^{\mu\nu} = 0$ , *i.e.*, it must be conserved (the expansion is done assuming that the lengthscales of the temperature and boost variations are much larger than the thermal lengthscale of the system). This stress tensor is found by computing the extrinsic curvature of a constant radial surface in the limit where this surface approaches the AdS boundary. The idea that the stress tensor must be conserved is certainly not new and was realized in previous studies of holographic descriptions of gravity as a quantum field theory on the boundary (namely in the AdS/CFT duality). However, with the exception of a few explicit examples, this stress tensor was *a priori* an arbitrary symmetric tensor in  $d$  dimensions with  $d(d+1)/2$  components (eventually  $d(d+1)/2 - 1$  if the quantum field theory on the boundary is conformal and thus traceless). These are too many degrees of freedom for the conservation equations to be closed. What is new with the boosted black brane patching and the perturbative analysis that follows is that in the process the form of the stress tensor is highly and uniquely constrained. For example, at leading order in the expansion it must have a perfect fluid form. This reduces strongly the degrees of freedom and the conservation equations now constitute a closed system: we have as many equations as unknowns. Moreover, there is also a one-to-one map between the bulk gravity solution and the boundary system. Working out the conservation equations we further find that they boil down to the equations of fluid dynamics.

These ideas were first developed to get a hydrodynamic description of AdS/CFT duality. However they naturally extend to other gravity/gauge theory dualities. Here we will be interested in dual systems that have a confinement/deconfinement phase transition [31, 32]. A particular example, that is the simplest one with these properties, is the Scherk-Schwarz (SS) gravity/gauge system [33, 34]. The reason to study such a system is (at least) two-folded. First, from a quantum field theory perspective, the SS gauge theory is non-supersymmetric, non-conformal and has the above mentioned phase transition. These are important properties that it shares with the real world QCD. Therefore the SS system can be a useful toy model to infer properties of QCD. In particular, having the gravity dual of the SS gauge theory we can use the fact that this is a weak/strong coupling duality to use the weak field gravity results to learn about the strong field (non-perturbative) regime of the field theory. Second, from a gravitational perspective, previous studies of the hydrodynamic SS system revealed an interesting but *a priori* unexpected feature [31]-[39][19]. SS AdS gravity differs from the globally AdS gravity (some of the main differences will be discussed in Section 4). However, results from SS hydrodynamics are telling us that black holes in this background have surprising similarities with globally AdS black holes or even asymptotically flat black holes. We can therefore use the SS hydrodynamic results to learn about these latter black holes in more conventional backgrounds.

Concretely, in the long wavelength regime, the SS compactification of a  $(d+1)$ -dimensional CFT has an effective description as a  $d$ -dimensional fluid dynamics with an equation of state that describes the SS plasma. This system is dual to the SS compactification of  $\text{AdS}_{d+2}$  gravity. In short, the SS theory has both a confined and a deconfined phase. In the gravity side of the duality the deconfined phase corresponds to a black hole solution localized in the infrared region of the holographic direction, while the confined phase maps to the AdS soliton solution. They compete

with each other for the minimal free energy. In the neighborhood of the confinement temperature the two phases co-exist in different regions of the spacetime and are separated by a domain wall whose tension provides the Israel junction conditions between the two solutions. In the holographic boundary where the fluid lives, the deconfined phase is described by a plasma lump immersed in the confined sea phase. The plasma lump has a surface tension at its boundary that is in correspondence with the domain wall tension in the bulk. For a more detailed description of this system we refer the reader to [32, 38].

For the present discussion, we should keep in mind that plasma lumps in  $d$ -dimensions correspond to SS  $\text{AdS}_{d+2}$  black objects. For example, axisymmetric plasma balls and plasma rings correspond, respectively, to rotating black holes and black rings in SS  $\text{AdS}_{d+2}$  [32]. In a previous study, rotating plasma balls were found to be unstable against  $m$ -lobed perturbations [38]. Starting with a static plasma ball and increasing its rotation, the axisymmetric rotating plasma ball becomes unstable first to a 2-lobed (“peanut-like”) perturbation and then to  $m$ -lobed perturbations with  $m > 2$ . This conclusion followed from analyzing perturbations of the hydrodynamic equations. Usually, such an instability signals a bifurcation point to a new branch of stationary solutions (that obeys the symmetries of the instability) in the phase diagram of stationary solutions. Here, we will find that this is indeed the case and we will construct explicitly the branch of 2-lobed plasma balls in the phase diagram of solutions.

The paper is organized as follows. Section 2 reviews the relativistic hydrodynamics of  $(2+1)$ -dimensional, stationary plasma configurations and displays the foundational equations for the remainder of the article. The main new results are contained in Section 3, where the non-axisymmetric profile of the  $m$ -lobed plasmas is found and the phase diagram for stationary plasmas is determined. For completeness, we briefly review the previously known results for axisymmetric solutions, both plasma balls and rings. In addition, we present a simple derivation that precludes the existence of  $m$ -lobed plasma rings as perturbations of axisymmetric plasma rings. We conclude in Section 4 with a discussion and some speculations on the gravitational duals of these plasma lumps. Appendix A contains an analysis of the non-relativistic limit.

## 2 Hydrodynamics of stationary plasma lumps

In this section we review the relativistic hydrodynamic equations that govern a Scherk-Schwarz plasma in a  $3d$  Minkowski background. We will be interested in plasma configurations in mechanical and thermodynamic equilibrium. This includes non-axisymmetric configurations. We discuss the conserved charges for stationary plasmas that allow to represent the branches of stationary plasmas in a phase diagram. We follow closely [36, 32].

### 2.1 Relativistic hydrodynamic equations

SS hydrodynamics is an effective description at long distances of SS gauge theory, valid when the fluid variables vary on distance scales that are large compared to the mean free path of the theory,  $l_{\text{mfp}} \sim 1/T_c$ . Expanding the holographic stress tensor  $T_{\mu\nu}$  in powers of derivatives of  $u^\mu$ , one finds that at leading order  $T_{\mu\nu}$  has a perfect fluid plus a surface tension boundary contributions, while the

dissipation effects due to shear and bulk viscosity plus heat diffusion appear in the next-to-leading order term.

The hydrodynamic equations follow from conservation of the stress tensor,  $\nabla_\mu T^{\mu\nu} = 0$ . This yields the relativistic continuity, Navier-Stokes and Young-Laplace equations,

$$u^\mu \nabla_\mu \rho + (\rho + P)\vartheta = \zeta \vartheta^2 - q^\mu a_\mu - \nabla_\mu q^\mu + 2\eta \sigma^{\mu\nu} \nabla_\mu u_\nu, \quad (2.1)$$

$$(\rho + P)a^\nu = -P^{\mu\nu} \nabla_\mu P + \zeta (P^{\mu\nu} \nabla_\mu \vartheta + \vartheta u^\mu \nabla_\mu u^\nu) + 2\eta (\nabla_\mu \sigma^{\mu\nu} - u^\nu \sigma^{\mu\alpha} \nabla_\mu u_\alpha) - (q^\mu \nabla_\mu u^\nu + \vartheta q^\nu + u^\mu \nabla_\mu q^\nu - q^\mu a_\mu u^\nu), \quad \text{with } P^{\mu\nu} \equiv g^{\mu\nu} + u^\mu u^\nu, \quad (2.2)$$

$$\left[ P - \zeta \vartheta + 2\eta \left( \frac{1}{2} \vartheta + u^\mu n^\alpha \nabla_\alpha n_\mu \right) \right]_{>}^{<} = \sigma K, \quad \text{with } K \equiv h_\mu{}^\nu \nabla_\nu n^\mu. \quad (2.3)$$

Here,  $u^\mu$  is the fluid velocity,  $\rho$ ,  $P$ ,  $\sigma$ ,  $\zeta$ ,  $\eta$  and  $\kappa$  are, respectively, the density, pressure, surface tension, bulk viscosity, shear viscosity, and thermal conductivity of the fluid. The quantities,  $a^\mu$ ,  $\vartheta$ ,  $\sigma^{\mu\nu}$  and  $q^\mu$  are respectively the acceleration, expansion, shear tensor, and heat flux.  $P^{\mu\nu}$  is the projector onto the hypersurface orthogonal to  $u^\mu$ . The fluid boundary is defined by  $f(x^\mu) = 0$ , it has unit spacelike normal  $n_\mu = \partial_\mu f / |\partial f|$ , and  $h^{\mu\nu} = g^{\mu\nu} - n^\mu n^\nu$  is the projector onto the boundary.  $K$  is the trace of its extrinsic curvature, and  $[Q]_{>}^{<} \equiv Q_{<} - Q_{>}$  is the jump on a quantity  $Q$  when we cross the boundary from the interior into the exterior of the plasma. In the derivation of (2.3), the constraint that the fluid velocity must be orthogonal to the boundary normal is used (this guarantees that the fluid is confined inside the boundary),

$$u^\mu n_\mu = 0. \quad (2.4)$$

A fluid with local entropy density  $s$  and local temperature  $\mathcal{T}$  satisfies the Euler relation and the Gibbs-Duhem relation given, respectively, by

$$\rho + P = \mathcal{T} s, \quad dP = s d\mathcal{T}, \quad (2.5)$$

In the SS dual system, we are interested in the long wavelength limit of a Scherk-Schwarz compactification of a 4-dimensional CFT. The 3d (non-conformal) plasma that results from the dimensional reduction of the 4d conformal plasma has equation of state [32]

$$P = \frac{\rho - 4\rho_0}{3} \iff \rho + P = \frac{4}{3}(\rho - \rho_0), \quad s = 4\alpha^{\frac{1}{4}} \left( \frac{\rho - \rho_0}{3} \right)^{\frac{3}{4}}, \quad \mathcal{T} = \left( \frac{\rho - \rho_0}{3\alpha} \right)^{\frac{1}{4}}. \quad (2.6)$$

with  $\rho_0$  and  $\alpha$  constants. This equation of state is valid in or out of equilibrium and is normalized such that the vacuum pressure vanishes.<sup>1</sup>

## 2.2 Stationary plasmas

In this subsection we briefly review some general results derived in [36] which are valid for equilibrium plasmas. For later sections, it is important to emphasize that these results are valid not only for axisymmetric but also for non-axisymmetric plasma configurations.

---

<sup>1</sup>The simplest possible plasma configuration - a domain wall separating the fluid from the vacuum - is in equilibrium when the plasma pressure vanishes. This occurs for a critical temperature  $\mathcal{T}_c = (\rho_0/\alpha)^{1/4}$  [32], or equivalently for a critical fluid density  $\rho_c = 4\rho_0$  for which  $P = 0$ .

Stationary plasma configurations are both in hydrodynamical,  $u^\mu \nabla_\mu P = 0$ , and thermodynamical equilibrium  $u^\mu \nabla_\mu \mathcal{T} = 0$ . Equivalently, they have  $\vartheta = 0$ ,  $\sigma^{\mu\nu} = 0$  and  $q^\mu = 0$ . Consequently, the velocity field of a stationary plasma must be a linear combination of the background Killing vector fields ( $\xi$  and  $\chi$  are the stationarity and rotational Killing vectors),

$$u = \frac{\mathcal{T}}{T} (\xi + \Omega \chi) . \quad (2.7)$$

In particular this implies that a stationary plasma must be at constant plasma temperature  $T$  related to the local temperature  $\mathcal{T}$  by the Lorentz factor

$$\gamma = \frac{\mathcal{T}}{T} = [-(\xi + \Omega \chi)^2]^{-1/2} , \quad (2.8)$$

which is the redshift factor relating measurements done in the laboratory and comoving frames. Combining the Euler relation (2.5) and the Young-Laplace equation (equation (2.3) without the dissipative terms), we can relate the plasma temperature  $T$  to a combination of several magnitudes at the fluid surface,

$$T = \frac{\sigma K + \rho}{\gamma s} . \quad (2.9)$$

In the plasma lump/black hole duality,  $T$  maps to the Hawking temperature of the horizon. A stationary plasma must also be rigidly rotating, *i.e.*, with constant angular velocity  $\Omega$ , which in turn maps to the horizon angular velocity in the duality.

Summarizing, the equations that a stationary fluid must satisfy are given by (2.1)-(2.3) with  $\vartheta = 0$ ,  $\sigma^{\mu\nu} = 0$  and  $q^\mu = 0$ . In particular the Young-Laplace equation (2.3) reduces to<sup>2</sup>

$$P_{<} - P_{>} = \sigma K . \quad (2.10)$$

For the SS plasma in equilibrium, it further follows from (2.8) and (2.6) that the pressure and energy density satisfy the relations

$$P = \frac{\rho_*}{3} \gamma^4 - \rho_0 , \quad \rho = \rho_* \gamma^4 + \rho_0 , \quad (2.11)$$

where  $\rho_* \equiv 3\alpha T^4$  is a constant for any given plasma configuration.

## 2.3 Conserved charges

The constituent fluid of the plasma object has local energy density  $\rho$ , pressure  $P$ , velocity  $u^\mu$ , local entropy density  $s$ , and local temperature  $\mathcal{T}$ . These *local* quantities provide the information we need to compute the thermodynamic quantities (energy, angular momentum, entropy, temperature) of the stationary configurations (plasma balls, plasma rings and plasma peanuts).

Here, we restrict our discussion to fluids that live in a (2+1)-dimensional Minkowski background<sup>3</sup> with stationarity timelike Killing vector  $\xi = \partial_t$  and spacelike Killing vector  $\chi = \partial_\phi$  (for

---

<sup>2</sup>The last term on the LHS of (2.10) vanishes in equilibrium because use of  $n^\mu n^\nu \sigma_{\mu\nu} = 0$  implies that  $u^\mu n^\alpha \nabla_\alpha n_\mu = n^\mu n^\alpha \nabla_\alpha u_\mu = 0$ .

<sup>3</sup>We use polar coordinates  $(t, r, \phi)$ , and the non-vanishing affine connections are  $\Gamma_{\phi\phi}^r = -r$  and  $\Gamma_{r\phi}^\phi = \Gamma_{\phi r}^\phi = 1/r$ .

general results see [36]). We can then foliate the spacetime into constant  $t$  hypersurfaces  $\Sigma_t$  and  $\xi^\mu$  is their unit normal vector. Then, given any Killing vector  $\psi^\mu$ , one can define the associated conserved charges  $\mathcal{Q}[\psi] = \int_{\Sigma_t} dV T_{\mu\nu} \xi^\mu \psi^\nu$ , where  $dV$  is the induced volume measure on  $\Sigma_t$ . The fluid velocity is given by (2.7), *i.e.*,  $u^\mu = \gamma (\delta^{\mu t} + \Omega \delta^{\mu \phi})$  with  $\gamma = (1 - r^2 \Omega^2)^{-1/2}$ . The energy and angular momentum of the plasma associated, respectively, with the Killing vectors  $\xi$  and  $\chi$  are then

$$\begin{aligned} E[V] &= \int_V [(\rho + P)(\xi \cdot u)^2 + (\xi \cdot \xi) P] dV - \sigma \int_{\Sigma_t} \xi^\mu \xi^\nu h_{\mu\nu} |\partial f| \delta(f) dV, \\ J[V] &= \int_V (\rho + P) (\xi \cdot u)(\chi \cdot u) dV - \sigma \int_{\Sigma_t} h_{\mu\nu} \xi^\mu \chi^\nu |\partial f| \delta(f) dV. \end{aligned} \quad (2.12)$$

Note that for axisymmetric solutions (plasma balls and plasma rings) the boundary term in  $J$  proportional to  $\sigma$  vanishes. It is however present for non-axisymmetric solutions where  $\chi \cdot n \neq 0$  (*i.e.*, when the fluid boundary is not invariant under the action of  $\chi$ ) [36]. The total entropy of the fluid is the conserved charge associated to the entropy density current  $su^\mu$ ,

$$S = - \int_V dV (\xi \cdot u) s = \int_V dV \gamma s. \quad (2.13)$$

### 3 Stationary solutions: balls, rings and lobed plasmas

In this section we are interested in rigidly rotating equilibrium configurations in a (2+1)-dimensional Minkowski background. In addition to the two families of axisymmetric solutions composed of plasma balls and plasma rings there exist also non-axisymmetric configurations or  $m$ -lobed plasmas, where  $m$  runs over the set of positive integers excluding 1. The plasma balls and rings were discussed in detail in [32]. Because we will later study the phase diagram of these solutions we review here their properties, following closely [32].

#### 3.1 Axisymmetric solutions: plasma balls and plasma rings

Consider plasma configurations in a 3d Minkowski background parametrized by coordinates  $(t, r, \phi)$ . The axisymmetry requirement demands that the boundaries of the plasma depend only on  $r$ . Each boundary is thus defined by the condition ( $\alpha$  specifies a particular boundary in the case where more than one is present)

$$f(r) = r - R_\alpha = 0, \quad (3.1)$$

and has unit normal  $n_\mu = \frac{\partial_\mu f}{|\partial f|} = \delta_{\mu r}$ . Its extrinsic curvature is  $K = \frac{1}{R_\alpha}$ . Following [32], it is convenient to frame our discussion in terms of the dimensionless variables,

$$\tilde{\Omega} = \frac{\sigma \Omega}{\rho_0}, \quad \tilde{r} = \frac{\rho_0 r}{\sigma}, \quad v = \Omega r = \tilde{\Omega} \tilde{r}, \quad (3.2)$$

and also to use dimensionless thermodynamic quantities,

$$\tilde{E} = \frac{\rho_0 E}{\pi \sigma^2}, \quad \tilde{J} = \frac{\rho_0^2 J}{\pi \sigma^3}, \quad \tilde{S} = \frac{\rho_0^{5/4} S}{\pi \alpha^{1/4} \sigma^2}, \quad \tilde{T} = T \left( \frac{\alpha}{\rho_0} \right)^{1/4}. \quad (3.3)$$

In 3d the possible axisymmetric stationary configurations are the plasma balls and the plasma rings:

- Plasma balls are characterized by having a single axisymmetric outer surface at  $r = R_o$  and by  $P_> = 0$ . Its properties can be found using the equation of state (2.11), and the Young-Laplace equation (2.10). It follows that plasma balls must satisfy the condition (with  $0 \leq v_o \leq 1$ )

$$\frac{\rho_*}{3\rho_0} = \left(1 + \frac{\tilde{\Omega}}{v_o}\right) (1 - v_o^2)^2. \quad (3.4)$$

- Plasma rings have an axisymmetric inner surface at  $r = R_i$  (where  $P_< = 0$ ), in addition to the outer surface at  $r = R_o$  (where  $P_> = 0$ ). The equation of state (2.11), and the Young-Laplace equation (2.10) introduce a constraint equation for these objects,

$$\left(1 + \frac{\tilde{\Omega}}{v_o}\right) (1 - v_o^2)^2 = \left(1 - \frac{\tilde{\Omega}}{v_i}\right) (1 - v_i^2)^2. \quad (3.5)$$

It constrains the three variables  $v_o$ ,  $v_i$  and  $\tilde{\Omega}$  as, *e.g.*,  $v_i = v_i(v_o, \tilde{\Omega})$ . An inspection of it concludes that there is a minimum  $v_o$ , call it  $v_o^*$ , above which (3.5) is valid [32]. So, plasma rings exist only for  $v_o \geq v_o^*$ . In fact there are two families of black rings. One is called the fat plasma ring and exists for  $\tilde{\Omega} \leq v_i \leq v_i^*$  (where  $v_i^* < v_o^*$  is such that the derivative of the RHS of (3.5) w.r.t.  $v_i$  vanishes). The second, dubbed as thin plasma ring, exists for  $v_i^* \leq v_i \leq 1$ . At  $v_i = v_i^*$  the two families meet at a regular solution. The condition  $v_i \geq \tilde{\Omega}$  guarantees that the temperature is non-negative.

The dimensionless energy, angular momentum and entropy of the plasma rings are, respectively,

$$\begin{aligned} \tilde{E} &= \frac{4(v_o^2 - v_i^2) - (v_o^4 - v_i^4) + 5\tilde{\Omega}(v_o + v_i) - \tilde{\Omega}(v_o^3 + v_i^3)}{\tilde{\Omega}^2}, \\ \tilde{J} &= \frac{2(v_o^4 - v_i^4) + 2\tilde{\Omega}(v_o^3 + v_i^3)}{\tilde{\Omega}^3}, \\ \tilde{S} &= \frac{4}{\tilde{\Omega}^2} \left[ v_o^2 \sqrt{1 - v_o^2} \left(1 + \frac{\tilde{\Omega}}{v_o}\right)^{3/4} - v_i^2 \sqrt{1 - v_i^2} \left(1 - \frac{\tilde{\Omega}}{v_i}\right)^{3/4} \right], \end{aligned} \quad (3.6)$$

and the corresponding charges for the plasma balls can be obtained from these formulas by taking  $v_i = 0$ .

## 3.2 Plasma peanuts and $m$ -lobed configurations

### 3.2.1 Boundary equation for lobed plasmas

According to the discussion in Section 2.2 the stationarity restriction can accommodate non-axisymmetric configurations as long as they are in rigid rotation. Taking this into account, we



drop the assumption of axisymmetry and define the surface of the plasma lump through the condition

$$f(t, r, \phi) \equiv r - R(t - \phi/\Omega) = 0. \quad (3.7)$$

The boundary's unit normal is

$$n_\mu = |\partial f|^{-1} \left( -R' \delta_\mu^t + \delta_\mu^r + \frac{R'}{\Omega} \delta_\mu^\phi \right), \quad |\partial f| = \left( \frac{\Omega^2 R^2 + R'^2 (1 - \Omega^2 R^2)}{\Omega^2 R^2} \right)^{\frac{1}{2}}, \quad (3.8)$$

where  $R' = \frac{dR(x)}{dx}$  with  $x = t - \phi/\Omega$ . The condition that no fluid flows through the surface, namely  $u^\mu n_\mu = 0$ , is manifestly satisfied by the ansatz (3.7) when the velocity field takes the form  $u^\mu = \gamma(\delta_t^\mu + \Omega \delta_\phi^\mu)$ . The trace of the extrinsic curvature of the boundary in the general rigid rotation case is

$$K = \Omega \frac{-RR'' (1 - \Omega^2 R^2) + R'^2 (2 - \Omega^2 R^2) + \Omega^2 R^2}{[\Omega^2 R^2 + R'^2 (1 - \Omega^2 R^2)]^{3/2}} \quad (3.9)$$

Introducing the dimensionless quantities (3.2) and

$$\psi = -\Omega x = \phi - \Omega t, \quad v_o(\psi) = \Omega R(x), \quad v'_o(\psi) = R'(x), \quad k = \frac{\rho_*}{3\rho_0}. \quad (3.10)$$

the Young-Laplace equation (2.3), after employing (2.6) and (2.8), becomes

$$\frac{v_o v_o'' (1 - v_o^2) - v_o'^2 (2 - v_o^2) - v_o^2}{[v_o^2 + v_o'^2 (1 - v_o^2)]^{3/2}} + \frac{1}{\tilde{\Omega}} [k(1 - v_o^2)^{-2} - 1] = 0. \quad (3.11)$$

This equation admits a first integral, namely the quantity

$$\frac{v_o^2}{\sqrt{v_o^2 + v_o'^2 (1 - v_o^2)}} - \frac{1}{2\tilde{\Omega}} [k(1 - v_o^2)^{-1} - v_o^2] \equiv Q \quad (3.12)$$

is a constant independent of  $\psi$ .

Now consider the stress tensor for a perfect fluid with surface tension  $\sigma$ . The relevant  $T_{\mu\nu}$  components to compute the charges are

$$\begin{aligned} T_{tt} &= \gamma^2 (\rho + \Omega^2 r^2 P) \Theta(-f) + \frac{\sigma}{\Omega R} \frac{\Omega^2 R^2 + R'^2}{\sqrt{\Omega^2 R^2 + R'^2 (1 - \Omega^2 R^2)}} \delta(f), \\ T_{t\phi} &= -\gamma^2 \Omega r^2 (\rho + P) \Theta(-f) - \sigma \frac{RR'^2}{\sqrt{\Omega^2 R^2 + R'^2 (1 - \Omega^2 R^2)}} \delta(f). \end{aligned} \quad (3.13)$$

The induced measure on a constant  $t$  hypersurface  $\Sigma_t$  used to compute the conserved charges in (2.12) and (2.13) is  $dV = r dr d\phi = \frac{\sigma^2}{\rho_0^2 \tilde{\Omega}^2} v dv d\psi$ . Using (2.12) and (2.13), the energy, angular momentum and entropy of the lobed plasma are then

$$\begin{aligned} \tilde{E} &= \frac{1}{2\pi \tilde{\Omega}^2} \int_0^{2\pi} d\psi \left[ v_o^2 + k \frac{v_o^2 (3 - v_o^2)}{(1 - v_o^2)^2} + 2\tilde{\Omega} \frac{v_o^2 + v_o'^2}{\sqrt{v_o^2 + v_o'^2 (1 - v_o^2)}} \right], \\ \tilde{J} &= \frac{1}{\pi \tilde{\Omega}^3} \int_0^{2\pi} d\psi \left[ \frac{k v_o^4}{(1 - v_o^2)^2} + \frac{\tilde{\Omega} v_o^2 v_o'^2}{\sqrt{v_o^2 + v_o'^2 (1 - v_o^2)}} \right], \\ \tilde{S} &= \frac{2}{\pi \tilde{\Omega}^2} \int_0^{2\pi} d\psi \frac{k^{3/4} v_o^2}{1 - v_o^2}, \end{aligned} \quad (3.14)$$

where  $v_o = v_o(\psi)$  is the velocity of the plasma peanut boundary that solves the Young-Laplace equation and  $v'_o = \frac{dv_o}{d\psi}$ . Note that by setting  $v'_o(\psi) = 0$ , and  $k = \left(1 + \tilde{\Omega}/v_o\right) (1 - v_o^2)^2$  (see (3.4)) we get the plasma ball charges (equation (3.6) with  $v_i = 0$ ).

Lobed plasma configuration are those whose boundary profiles satisfy equation (3.11) (or (3.12)). Next we find these solutions in a perturbative expansion around the plasma ball bifurcation point.

### 3.2.2 Lobed plasmas from perturbed analysis of plasma balls

As a warm-up exercise that will also be very useful to check our numerical results against, we find lobed plasma configurations by performing a perturbative analysis of the plasma balls around the bifurcation point to the new phase.

Consider a small non-axisymmetric perturbation of the plasma ball,

$$\begin{aligned} v_o(\psi) &= \hat{v}_o [1 + \varepsilon \nu(\psi) + \mathcal{O}(\varepsilon^2)] , \\ \tilde{\Omega} &= \hat{\Omega} + \varepsilon \omega + \mathcal{O}(\varepsilon^2), \quad k = \hat{k} + \varepsilon \kappa + \mathcal{O}(\varepsilon^2). \end{aligned} \quad (3.15)$$

where the hat refers to the (constant) unperturbed quantities,  $\varepsilon \ll 1$  is the expansion parameter, and the unperturbed plasma ball radius  $\hat{v}_o$  necessarily obeys (3.4), which we write here as

$$\hat{\Omega} = \hat{v}_o [\hat{k}(1 - \hat{v}_o^2)^{-2} - 1] . \quad (3.16)$$

Note that a consistent perturbation requires that we disturb not only  $v_o$  but also  $\tilde{\Omega}$  and  $k$ , as done in (3.15). Linearizing the Young-Laplace equation (3.11) we then get

$$\nu'' + m^2 \nu = \Delta , \quad (3.17)$$

with

$$m^2 = \frac{1}{1 - \hat{v}_o^2} + \frac{4\hat{k}\hat{v}_o^3}{\hat{\Omega}(1 - \hat{v}_o^2)^4}, \quad \Delta = \hat{v}_o \frac{[\hat{k} - (1 - \hat{v}_o^2)^2] \omega - \hat{\Omega} \kappa}{\hat{\Omega}^2 (1 - \hat{v}_o^2)^3} . \quad (3.18)$$

The solution for the perturbation is oscillatory,

$$\nu(\psi) = A \sin(m\psi + \beta) + \Delta/m^2, \quad (3.19)$$

and imposing periodicity  $\psi \rightarrow \psi + 2\pi$  implies that  $m \in \mathbb{Z}$ . The plasma peanuts correspond to  $m = 2$ . The definition of the small expansion parameter,

$$\varepsilon \equiv \frac{1}{\hat{v}_o} \int_0^\pi d\psi [v_o(\psi) - \hat{v}_o] \nu(\psi), \quad (3.20)$$

provides a normalization for the function  $\nu(\psi)$ :

$$\int_0^\pi d\psi [\nu(\psi)]^2 = 1. \quad (3.21)$$

This in turn may be used to fix the amplitude  $A$  as

$$A = \sqrt{\frac{2}{\pi} \left(1 - \frac{\pi \Delta^2}{m^4}\right)}. \quad (3.22)$$

However,  $A$  does not enter the first order expansions of the various thermodynamic quantities so we shall not need it.

Note that combining eqs. (3.16) and (3.18) we obtain the constraint

$$m^2 = \frac{1 + 3\hat{v}_o^2 + 4\hat{v}_o^3/\hat{\Omega}}{(1 - \hat{v}_o^2)^2}. \quad (3.23)$$

Recall that for a given energy, the unperturbed plasma ball quantities  $\hat{v}_o$  and  $\hat{\Omega}$  are related by the first equation in (3.6). Relation (3.23) then determines the value of  $\hat{v}_o$  (or  $\hat{\Omega}$ ) where the  $m$ -lobed plasma bifurcates from the plasma ball branch for a given energy. In the non-relativistic limit,  $\hat{v}_o \ll 1$  and  $\frac{\sigma}{\rho_0 R_o} \ll 1$ , eq. (3.23) reduces to  $4R_o^3 \Omega^2 \rho_0 / \sigma = m^2 - 1$  and agrees with the bifurcation point found in [38].<sup>4</sup>

Having identified the bifurcation point we can now determine the slope of the new phase branch curve in the neighborhood of the bifurcation point. Expanding to first order the dimensionless energy, angular momentum and entropy of the lobed plasmas (given by eq. (3.14)) around the plasma balls, we get

$$\begin{aligned} \tilde{E} &= \tilde{E}_{pb} + \varepsilon \frac{\hat{v}_o^2}{\hat{\Omega}^2} \left\{ \frac{3 - \hat{v}_o^2}{(1 - \hat{v}_o^2)^2} \kappa - \frac{2}{\hat{\Omega}} \left[ \left( 1 + \frac{\hat{\Omega}}{\hat{v}_o} \right) + \frac{\hat{k}(3 - \hat{v}_o^2)}{(1 - \hat{v}_o^2)^2} \right] \omega + \left[ \left( 1 + \frac{\hat{\Omega}}{\hat{v}_o} \right) + \frac{\hat{k}(3 + \hat{v}_o^2)}{(1 - \hat{v}_o^2)^3} \right] \frac{2\Delta}{m^2} \right\} \\ &\quad + O(\varepsilon^2), \\ \tilde{J} &= \tilde{J}_{pb} + \varepsilon \frac{\hat{k} \hat{v}_o^4}{\hat{\Omega}^3 (1 - \hat{v}_o^2)^2} \left\{ \frac{2\kappa}{\hat{k}} - \frac{6\omega}{\hat{\Omega}} + \frac{8\Delta}{m^2 (1 - \hat{v}_o^2)} \right\} + O(\varepsilon^2), \\ \tilde{S} &= \tilde{S}_{pb} + \varepsilon \frac{\hat{k}^{3/4} \hat{v}_o^2}{\hat{\Omega}^2 (1 - \hat{v}_o^2)} \left\{ \frac{3\kappa}{\hat{k}} - \frac{8\omega}{\hat{\Omega}} + \frac{8\Delta}{m^2 (1 - \hat{v}_o^2)} \right\} + O(\varepsilon^2). \end{aligned} \quad (3.24)$$

Here, the subscript  $pb$  is appended to quantities pertaining to plasma balls (see eq. (3.6) for their definitions).

In the next subsection we shall obtain the phase diagram at fixed energy. Since we focus on 2-lobed perturbations of plasma balls, we require that the energy  $\tilde{E}$  of the non-axisymmetric configuration actually equals  $\tilde{E}_{pb}$ . Thus, the energy constraint reads

$$\frac{3 - \hat{v}_o^2}{(1 - \hat{v}_o^2)^2} \kappa - \frac{2}{\hat{\Omega}} \left[ \left( 1 + \frac{\hat{\Omega}}{\hat{v}_o} \right) + \frac{\hat{k}(3 - \hat{v}_o^2)}{(1 - \hat{v}_o^2)^2} \right] \omega + \left[ \left( 1 + \frac{\hat{\Omega}}{\hat{v}_o} \right) + \frac{\hat{k}(3 + \hat{v}_o^2)}{(1 - \hat{v}_o^2)^3} \right] \frac{2\Delta}{m^2} = 0. \quad (3.25)$$

Together with (3.18), the energy constraint yields a linear relation between the first-order perturbation quantities,

$$\kappa = \omega \frac{(1 - \hat{v}_o^2)^2 (9 - 39\hat{v}_o^2 + 54\hat{v}_o^4 - 27\hat{v}_o^6 + 4\hat{v}_o^8)}{\hat{v}_o (-3 + 10\hat{v}_o^2 - 8\hat{v}_o^4 + 2\hat{v}_o^6)}, \quad (3.26)$$

---

<sup>4</sup>There is an interesting feature associated with this value. In [38] the classical critical rotation was found studying perturbations of the dissipative hydrodynamic equations (2.1)-(2.3) in their non-relativistic limit. Curiously, if we repeat the perturbation analysis starting this time with the *non*-dissipative fluid equations we find that the value of the critical rotation *shifts* to  $4R_o^3 \Omega^2 \rho_0 / \sigma = m(m+1)$ . So, even a vanishingly small viscosity has a dramatic effect on the critical rotation at which instability sets in. Viscosity introduces a singular-limit, where the “limit of the theory is not the theory of the limit”. In classical fluids this property is very familiar and well studied [40, 41].

where we have used eqs. (3.16) and (3.23) to eliminate  $\widehat{k}$  and  $\widehat{\Omega}$  in favor of  $\widehat{v}_o$  (and replaced  $m = 2$ ).

At this point we have not yet fully determined the first-order quantities  $\{\nu(\psi), \omega, \kappa\}$ , but to compute the slope at which the plasma peanut branches off from the plasma ball curve in the  $\widetilde{S} - \widetilde{J}$  phase diagram we need not go further<sup>5</sup>. The reason for this is that the slope (at the bifurcation point) is given by

$$\left(\frac{\partial \widetilde{S}}{\partial \widetilde{J}}\right)_{\widetilde{E}}^{\text{peanut}} = \lim_{\varepsilon \rightarrow 0} \frac{\left(\frac{\partial \widetilde{S}}{\partial \varepsilon}\right)_{\widetilde{E}}}{\left(\frac{\partial \widetilde{J}}{\partial \varepsilon}\right)_{\widetilde{E}}}, \quad (3.27)$$

and therefore the only terms for  $\widetilde{S}$  and  $\widetilde{J}$  in eq. (3.24) that contribute are those linear in  $\varepsilon$ . Taking the ratio, the undetermined first-order quantity that was left cancels out, leaving an expression as a function of  $\widehat{v}_o$  only. The final result for the slope of the plasma peanut at the bifurcation point in the  $\widetilde{S}(\widetilde{J})$  phase diagram is

$$\left(\frac{\partial \widetilde{S}}{\partial \widetilde{J}}\right)_{\widetilde{E}}^{\text{peanut}} = -\frac{4\widehat{v}_o^3}{(3 - 4\widehat{v}_o^2)^{1/4} [(1 - \widehat{v}_o^2)(3 - 11\widehat{v}_o^2 + 4\widehat{v}_o^4)]^{3/4}}. \quad (3.28)$$

For  $\widetilde{E} = 40$ , eqs. (3.6) and (3.23) determine the bifurcation point to occur at  $\widehat{v}_o \simeq 0.378$  ( $\widehat{\Omega} \simeq 0.14$ ). Plugging this value into eq. (3.28) we obtain  $\partial \widetilde{S} / \partial \widetilde{J} \simeq -0.142$ . This perturbative result will be compared with the numerical result of the next subsection and a good agreement will be found.

### 3.2.3 Phase diagram of stationary plasmas

We have integrated numerically equation (3.11) to find lobed-like solutions. In the numerical search, we fix the energy at  $\widetilde{E} = 40 \pm 10^{-7}$  (for simplicity, since it allows comparison with previous investigations [32, 35, 38]), and vary  $\widetilde{\Omega}$ . There are three parameters to be varied in the numerical integration:  $\widetilde{\Omega}$ ,  $k$  and  $v_o(0)$ . For each  $\widetilde{\Omega}$ , we search for an array of  $k, v_o(0)$ , which yield  $m$ -lobed solutions with  $v_o(0)/v_o(2\pi) = 1 \pm 10^{-7}$ . Among those, we select the one for which  $\widetilde{E} = 40 \pm 10^{-7}$ . We started the integration close to the plasma ball configuration, by looking for a two-lobed solution with  $v_o(0) \sim v_o(\pi)$ . We find that the bifurcation to plasma peanuts occurs at the critical values  $\widetilde{J} \simeq 22.2$ ,  $\widetilde{\Omega} \simeq 0.16$ ,  $\widetilde{S} \simeq 32.7$ , and  $\widetilde{T} \simeq 1.0$ . Our results are summarized in Figures 1-2.

In Figure 1, we show typical two-lobed configurations for different values of rotation parameter,  $\widetilde{\Omega} \sim 0.13, 0.12, 0.09$  respectively. As  $\widetilde{\Omega}$  decreases, the configurations get more and more distorted, and for small rotations they assume the form of peanut-like shapes, as in the rightmost panel of Figure 1. Once one knows the configuration shape it is straightforward to compute the energy, entropy and angular momentum from eqs. (3.24) and to establish the phase diagrams  $\widetilde{S}(\widetilde{J})$ ,  $\widetilde{\Omega}(\widetilde{J})$  and  $\widetilde{T}(\widetilde{J})$ . These diagrams are shown in Figure 2, where we include also plasma balls and plasma rings [32]. For the particular energy we are considering, the 2-lobed configurations have a slope of about  $\partial \widetilde{S} / \partial \widetilde{J} \sim -0.149$ . This is in very good agreement ( $\sim 5\%$ ) with the perturbative construction prediction  $\partial \widetilde{S} / \partial \widetilde{J} \simeq -0.142$  of the last subsection. We have constructed numerically other configurations, including classical configurations, for which the velocities are very small, and we have obtained good agreement for the slopes predicted in [38].

---

<sup>5</sup>In the non-relativistic case the perturbative analysis must be extended to second order [38].

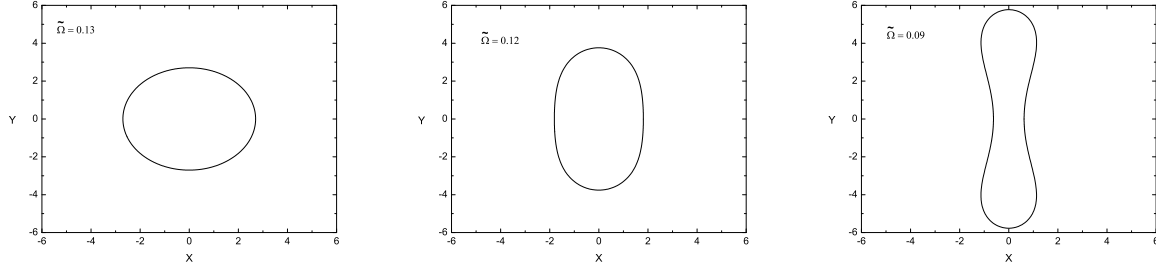


Figure 1: Different configurations of a two-lobed plasma for three different values of angular velocity  $\tilde{\Omega} = 0.13, 0.12, 0.09$ . The energy is kept fixed at  $\tilde{E} = 40$  and the bifurcation rotation occurs at  $\tilde{\Omega} \simeq 0.16$ . (The rotation axis is normal to the page).

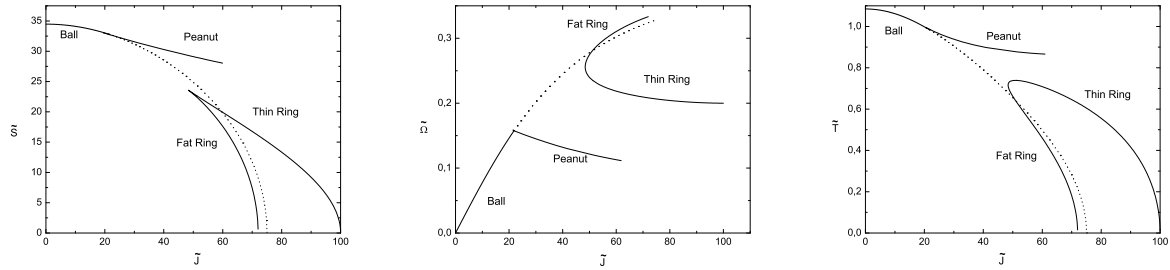


Figure 2: Phase diagrams  $\tilde{S}(\tilde{J})$ ,  $\tilde{\Omega}(\tilde{J})$  and  $\tilde{T}(\tilde{J})$  with the two-lobed, “peanut-like” configurations, along with the plasma balls, and thin and fat plasma rings found in [32]. The energy is fixed at  $\tilde{E} = 40$  as in [32].

One particularity of the plasma peanuts (common to the thin rings) may be noted here: for these configurations an increase of angular momentum produces a *decrease* of angular velocity, as is evident from Figure 2. Such a phenomenon is made possible because the moment of inertia grows accordingly and this is apparent in Figure 1.

### 3.3 No $m$ -lobed plasma rings

A natural question that emerges from the plasma ball analysis done so far is whether or not it is possible to have also  $m$ -lobed plasma rings. In a previous study this question was addressed by perturbing hydrodynamic equations (2.1)-(2.3) with an ansatz that satisfied the symmetries of the hypothetical  $m$ -lobed plasma rings [38]. The analysis concluded that plasma rings are stable against this particular sector of perturbations. We now revisit this problem from a different perspective. The outcome of the present analysis will reinforce the conclusion of the previous study.

Motivated by the success of the analysis done in subsection 3.2.2, the idea is to ask if we can get  $m$ -lobed plasma rings as perturbative solutions around a possible bifurcation point in the plasma ring branch. It follows from the Young-Laplace equation (2.10) and equilibrium equation of state (2.11) that the outer boundary of a hypothetical  $m$ -lobed plasma ring has to satisfy (3.11), and its inner boundary must obey a similar relation with the trade  $v_o \rightarrow v_i$  for fixed  $\{k, \tilde{\Omega}\}$ . The fact that the parameter  $k = \rho_*/(3\rho_0)$  must be the same for both boundaries in particular implies that such

a solution would have to satisfy the relation,

$$\begin{aligned} k &= (1 - v_o^2)^2 \left( 1 - \tilde{\Omega} \frac{v_o v_o''(1 - v_o^2) - v_o'^2(2 - v_o^2) - v_o^2}{[v_o^2 + v_o'^2(1 - v_o^2)]^{3/2}} \right) \\ &= (1 - v_i^2)^2 \left( 1 - \tilde{\Omega} \frac{v_i v_i''(1 - v_i^2) - v_i'^2(2 - v_i^2) - v_i^2}{[v_i^2 + v_i'^2(1 - v_i^2)]^{3/2}} \right). \end{aligned} \quad (3.29)$$

In the axisymmetric case,  $v_o' = 0 = v_i'$ , this relation reduces to the equilibrium condition (3.5).

Consider now the (natural) possibility that an  $m$ -lobed plasma ring could emerge from a slight perturbation of an axisymmetric plasma ring. Following a similar strategy as in section 3.2.2, we linearize (3.29) by perturbing the boundaries as

$$v_\alpha(\psi) = \hat{v}_\alpha [1 + \varepsilon \nu_\alpha(\psi) + \mathcal{O}(\varepsilon^2)] , \quad \text{with } \alpha = o, i, \quad (3.30)$$

and  $\tilde{\Omega}$  and  $k$  as in (3.15). Again, the hat refers to the (constant) unperturbed quantities. To leading order, we get (3.5) and in the next-to-leading order we find the two equations,

$$\nu_\alpha'' + m_\alpha^2 \nu_\alpha = \Delta_\alpha, \quad \text{with } \alpha = o, i, \quad (3.31)$$

and

$$m_\alpha^2 = \frac{1}{1 - v_\alpha^2} + \epsilon_\alpha \frac{4 \hat{k} \hat{v}_\alpha^3}{\hat{\Omega} (1 - \hat{v}_\alpha^2)^4}, \quad \Delta_\alpha = \epsilon_\alpha \hat{v}_\alpha \frac{[\hat{k} - (1 - \hat{v}_\alpha^2)^2] \omega - \hat{\Omega} \kappa}{\hat{\Omega}^2 (1 - \hat{v}_\alpha^2)^3}, \quad \epsilon_{o,i} \equiv \pm 1. \quad (3.32)$$

Each of these equations admits an oscillatory solution of the form (3.19).  $m$ -lobed plasma rings can exist only if the number of nodes in the outer and inner boundaries is the same, *i.e.*, if the condition

$$m_o = m_i, \quad m_o, m_i \in \mathbb{Z} \quad (3.33)$$

is satisfied. In this relation and (3.32), the unperturbed quantities are constrained as discussed in subsection 3.1, *e.g.*, one must have  $\hat{\Omega} \leq \hat{v}_i \leq 1$  and  $\hat{k} = \hat{k}(\hat{\Omega}, \hat{v}_o) = \hat{k}(\hat{\Omega}, \hat{v}_i)$  as indicated in (3.5). An inspection of (3.32) concludes that the equality (3.33) is verified only when  $\hat{v}_i \geq \hat{v}_o$  (see Fig. 3). This clearly violates the basic assumption that the inner radius of the plasma ring must be smaller than its outer radius.

This analysis therefore rules out the possibility that lobed plasma rings could exist as a branch of solutions emerging perturbatively from the axisymmetric plasma rings. There is a clear physical reason for why the plasma rings are stable against “lobing”, in contradiction with plasma balls. The additional angular momentum acts to push the fluid radially outward. For the plasma ball the only way this can be done while preserving the energy is by breaking axial symmetry, whereas plasma rings can accommodate such a change by becoming larger and thinner<sup>6</sup>.

Reference [38] looked for the possible existence of these solutions following a different path. It analyzed the stability of a plasma ring against  $m$ -lobed perturbations such that these were in phase both in the inner and outer boundary deformations. No unstable mode was found. These two negative results following different approaches seem to suggest that the existence of  $m$ -lobed plasma rings is ruled out.

---

<sup>6</sup>This argument is due to V. Hubeny, to whom we thank.

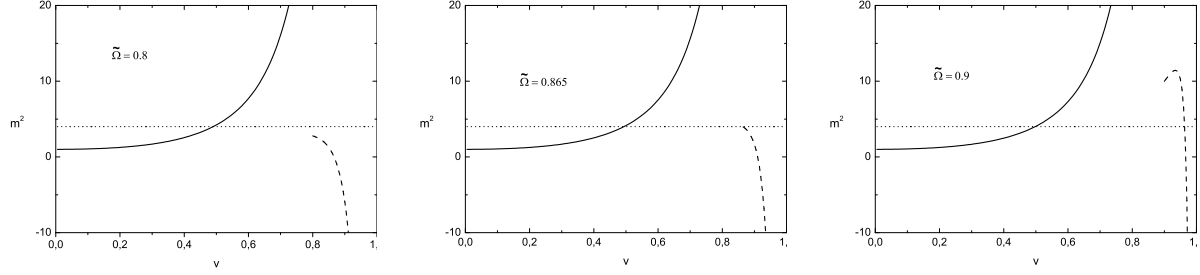


Figure 3:  $m^2$  as a function of  $v_\alpha$  for the three possible regimes of  $\tilde{\Omega}$ . The solid line represents  $m_o^2(\tilde{\Omega}, \hat{v}_o)$ , while the dashed line represents  $m_i^2(\tilde{\Omega}, \hat{v}_i)$ . The case  $m_o = m_i = 2$  is possible only for large rotations and when  $\hat{v}_i \geq \hat{v}_o$ . This violates the plasma ring condition that the inner radius must be smaller than the outer radius.

### 3.4 The hydrodynamic regime

Relativistic hydrodynamics provides a good effective description of the deconfined plasma phase of  $\mathcal{N} = 4$  Yang Mills theory compactified down to  $d = 3$  on a Scherk-Schwarz circle only if certain conditions are satisfied [32]. First, hydrodynamics is by definition valid when the thermodynamic quantities of the fluid vary on a lengthscale large when compared with the mean free path,  $\ell_{\text{mfp}}$ , of fluid constituent particles. In our case  $\ell_{\text{mfp}} \sim T_c^{-1} \sim \frac{\sigma}{\rho_0}$ . A good estimate for the valid regime is obtained when the maximum fractional rate of change of the fluid local temperature,  $\frac{\delta T}{T}|_{\text{max}} \sim \partial_r \ln \gamma|_{\text{max}}$  (recall that  $\mathcal{T} = T\gamma$ ) is much smaller than  $\ell_{\text{mfp}}^{-1}$ . This occurs for  $\frac{\Omega v_o}{1-v_o^2} \ll 1$ . This condition is satisfied by a wide range of plasma balls and rings as long as we are away from extremality [32]. Second, the analysis done so far and onwards assumes that surface tension is constant,  $\sigma = \sigma(T_c)$ , when in fact it is a function of the fluid temperature at the surface. This assumption is valid when  $\mathcal{T}/T_c \sim 1$  at the boundary surfaces. This is the case for an extended range of energies and angular momenta as long as we do not approach the extremal configurations [32] too closely. Finally, the boundary of the plasma is treated as a delta-like surface when in fact it has a thickness of order  $T_c^{-1}$ . So the analysis is valid when the boundary radius is everywhere large when compared with  $T_c^{-1}$ ,  $\{R_o, R_i, R_o - R_i\} \gg \frac{\sigma}{\rho_0}$ . This is satisfied if the plasma energy is large and again if we are away from the extremal configurations [32].

## 4 Gravity duals. Discussion

Since plasma balls are unstable above a critical rotation rate, the holographic dual SS AdS<sub>5</sub> black holes should also be unstable against  $m$ -lobed perturbations. This instability then provides a mechanism that dynamically bounds the rotation of these black holes. From the plasma results, we expect this bound to be well below the rotation where the extreme solution is reached (for which  $\tilde{T} = 0$ ), and below the minimal rotation where SS AdS<sub>5</sub> black rings can exist. Very little is known about SS AdS<sub>5</sub> black holes, so we are unable at this point to explicitly check the existence of this instability and rotation bound in the gravitational system.

In the fluid, we explicitly found the new branch of stationary non-axisymmetric plasmas bi-

furcating from the plasma ball curve at the point where the instability becomes active. In the simplest  $m = 2$  case this is a plasma peanut. In the entropy *vs* angular momentum diagram (for fixed mass) the plasma peanuts have higher entropy than the plasma ball. In fact, for the range of angular momenta for which plasma peanut solutions exist, they are entropically dominant over all the stationary configurations.

In the dual gravitational system,  $m$ -lobed plasma balls are in correspondence with  $m$ -lobed black holes. However, the latter can only exist as a long lived object, but never as a stationary solution. Indeed, a rotating non-axisymmetric black hole has a quadrupole moment and thus necessarily radiates away its lobed deformations<sup>7</sup>. The expectation is that this emission of gravitational waves will proceed until the system is back to an axisymmetric configuration spinning at a rate below the critical rotation where the instability kicks in.

This point deserves a few more words. Consider first global  $\text{AdS}_{d+2}$  spacetime. Its boundary is the Einstein static universe  $\mathbb{R}_t \times S^d$ . This boundary behaves effectively as a reflecting wall or box. Therefore, in this background one could eventually have a spinning non-axisymmetric black hole surrounded by rotating radiation. The rate at which the black hole would be radiating could in principle be balanced by the absorption of previously emitted radiation that is reflected from the boundary. An equilibrium solution with a black hole plus orbiting radiation is *a priori* conceivable in this background. On the other hand, SS AdS has boundary  $\mathbb{R}_t \times \mathbb{R}^{d-1} \times S^1_{SS}$  and behaves quite differently. In this background, only propagation along the holographic radial direction faces reflective boundary conditions. Along the other spacelike directions, namely those parallel to the holographic boundary (where the dual fluid lives), we have asymptotically flat boundary conditions. It then follows that waves emitted by a black hole along the radial direction will be reflected back but radiation emitted along the boundary directions will leak towards infinity. Therefore, the  $m$ -lobed plasma balls are dual to long-lived lobed SS AdS black holes that decay slowly, *i.e.*, that loose angular momentum along the boundary directions and cannot be stationary.

The existence of the lobed instability and of the stationary plasma peanuts and related families exposes the need to explore one point in the fluid/gravity correspondence that is still poorly understood: what is the fluid description of gravitational interactions and gravitational radiation? At the approximation level at which the duality is currently understood, hydrodynamics can only describe gravitational systems where these phenomena are suppressed. Indeed, two plasma balls do not interact, their collision is not accompanied by radiation emission and a non-axisymmetric plasma ball does not radiate. In short, the fluid description only captures the interaction of two black holes in the limit when their separation is much larger than the AdS radius, and the gravitational emission in the limit where its wavelength is much larger than the AdS scale.

It is known that the gravitational radiation and interaction corresponds in the plasma to the emission of glueballs. It is also known that in the large  $N$  limit of confining  $SU(N)$  gauge theories that have a gravitational dual, the energy loss in this emission process is suppressed by a  $1/N^2$  factor when compared with the plasma ball energy density. For this reason we know that our plasma results describe a necessarily long-lived SS AdS lobed black hole where gravitational emission occurs at a very slow rate. It would nevertheless be very interesting to work out more quantitatively the

---

<sup>7</sup>A static non-axisymmetric black hole was argued to exist in Kaluza-Klein gravity, *i.e.*, that asymptotes to  $M^d \times S^1$ , for  $d \geq 4$  [42].



fluid description of the gravitational emission and interaction processes, to accommodate also in the formulation cases where these phenomena are not suppressed. However, it is conceivable that such processes might force one to leave the regime of validity of the hydrodynamic description and therefore may be hard to capture<sup>8</sup>.

Although we have only worked out the lowest dimensional case, higher dimensional SS AdS theories also have a fluid description. More specifically, for any  $d \geq 3$ , the SS compactification of  $(d + 1)$ -dimensional CFT has a  $d$ -dimensional fluid dynamic description which is dual to a SS compactification of  $\text{AdS}_{d+2}$ . An interesting evolution is expected as we climb the dimension ladder. As described above, the asymptotics of SS AdS gravity roughly interpolates between AdS and Minkowski asymptotics depending on the spatial direction we look at. But as we increase the number of dimensions the “AdS-like” radial direction is kept and we are only adding more and more “flat-like” boundary directions. Therefore, we anticipate that as  $d$  grows the fluid results should describe black holes whose properties increasingly resemble those of asymptotically flat black holes [36, 39]. The known results confirm this expectation, as we briefly review next. Start with  $d = 3$ . The phase diagram for plasma balls and plasma rings in  $3d$  (see Figure 2) is similar to the phase diagram expected for black holes and black rings in  $\text{AdS}_5$  [32]. In particular, in contrast to the asymptotically flat solutions, the black rings have an upper bound on the rotation above which they would not fit in the AdS box [32]. So, the  $3d$  plasma results indicate that the SS  $\text{AdS}_5$  black objects behave similarly to  $\text{AdS}_5$  black holes. When we increase the dimension by one unit two interesting new features emerge [32, 35]. (The following discussion only highlights some properties of interest for our purpose; we ask the reader to see [35] for details). First, the plasma rings have now unbounded angular momentum. That is, SS  $\text{AdS}_6$  black rings behave much like  $6d$  asymptotically flat black rings. So, quite amazingly, in what concerns this particular feature in the fluids  $d = 4$  sets already the critical dimension for the above mentioned transition between an asymptotically AdS and asymptotically flat behavior. Second, from the gravitational perspective, we know that asymptotically flat (singly spinning) black holes in  $d \geq 6$  have no bound on their rotation. The transition from moderately rotating black holes into ultraspinning ones is set by the critical rotation where the so-called ultraspinning instability becomes active [45, 46]<sup>9</sup>. In the phase diagram of solutions this marks a bifurcation point to a new branch of axisymmetric pinched black holes whose horizon is distorted with ripples along the polar direction. Returning to the fluid results, in  $d = 4$  a third stationary solution – the pinched plasma balls – is indeed found, in addition to the plasma balls and rings [32, 35].

We have not worked out the technical details but in  $d > 3$  the  $m$ -lobed instability must also be present in the plasma balls. The reason being that it is well established that unstable phenomena

---

<sup>8</sup>We thank M. Rangamani for pointing this out to us.

<sup>9</sup>In more detail, when rotation keeps increasing in the ultraspinning regime the horizon flattens in the neighborhood of the axis poles and the geometry becomes more and more like the geometry of a black membrane [45]. But the latter is unstable against the Gregory-Laflamme instability when their length along the extended directions is bigger than their transverse radius [43]. Therefore, at the critical rotation where we enter the ultraspinning regime (and well below the limit where the geometry becomes a black membrane) the rotating black holes are expected to become unstable against the naturally dubbed ultraspinning instability [45]. A recent study confirmed that this is indeed the case [46]. In the fluid description, the Gregory-Laflamme instability maps into the Rayleigh-Plateau instability that is responsible for the pinch-off of long plasma tubes or branes into plasma balls [44, 36].

that are already present in classical fluid dynamics cannot cease to exist in relativistic hydrodynamics. Now, in [47] it was found that the lobed instability is indeed active in higher dimensional classical fluids. Therefore it should persist in the relativistic regime. The interesting question is then whether this instability appears at lower or higher values of rotation than the ultraspinning one. We argue that it should appear for lower spins. The argument is simple but seems to be robust: in  $3d$  the former instability is present while the latter does not appear. It would become active at rotations higher than the upper bound for the angular momentum. When we increase  $d$  this cap in  $J$  disappears and the ultraspinning makes its appearance but, it should do so at a rotation larger than the 2-lobed critical rotation.

As emphasized several times, the plasma results are strictly dual to SS AdS gravity. But as described above, in certain regimes, we also have or expect strong similarities between black holes in this background and those that are globally AdS or asymptotically flat. It is therefore compelling to conjecture the possibility that a non-axisymmetric  $m$ -lobed instability might also be present in higher dimensional Myers-Perry(–AdS) black holes. We do not find any reason to discard it *a priori*; a numerical investigation of this hypothetical instability might reveal interesting results.

## Acknowledgments

We warmly thank Marco Caldarelli and R. Loganayagam for very fruitful discussions, and specially Veronika Hubeny and Mukund Rangamani for their useful comments to the final version of this manuscript. OJCD thanks the organizers and participants of the *Workshop on Fluid-Gravity Correspondence*, University Ludwig-Maximilians of Munich, Germany, for wonderful hospitality and discussions. OJCD acknowledges financial support provided by the European Community through the Intra-European Marie Curie contract PIEF-GA-2008-220197. JVR acknowledges financial support from *Fundação para a Ciência e Tecnologia* (FCT)-Portugal through fellowship SFRH/BPD/47332/2008. This work was partially funded by FCT-Portugal through projects PTDC/FIS/64175/2006, PTDC/FIS/098025/2008, PTDC/FIS/098032/2008, CERN/FP/ 83508/2008. The authors thankfully acknowledge the computer resources, technical expertise and assistance provided by the Barcelona Supercomputing Center - Centro Nacional de Supercomputacin.

## Appendix

### A Non-relativistic lobed configurations

In this Appendix we review the classical hydrodynamic equations that describe non-relativistic fluids and, in particular, lobed configurations [48]-[50]. As a consistency check, we confirm that the non-relativistic (NR) limit of our equations for the plasma peanuts reduces to these classical equations.

The classical analysis of rigidly rotating fluids is standardly done in the rotating frame of reference. The advantage of this frame is that the (unperturbed) velocity of the fluid vanishes. In this frame, the classical Navier-Stokes, continuity and Young-Laplace equations are respectively

given by

$$\begin{aligned}
\partial_t \mathbf{v} + (\mathbf{v} \cdot \bar{\nabla}) \mathbf{v} &= -\frac{1}{\rho} \bar{\nabla} P - 2\boldsymbol{\Omega} \times \mathbf{v} + \frac{1}{2} \bar{\nabla} (|\boldsymbol{\Omega} \times \mathbf{r}|) , \\
\partial_t \rho + \mathbf{v} \cdot \bar{\nabla} \rho + \rho \bar{\nabla} \cdot \mathbf{v} &= 0 , \\
P_{<} - P_{>} &= \sigma \bar{K} , \quad \text{with } \bar{K} \equiv \bar{\nabla} \cdot \mathbf{n} ,
\end{aligned} \tag{A.1}$$

where  $\mathbf{v}$  is the spatial fluid velocity, and  $\bar{\nabla}$  the spatial gradient. In the Navier-Stokes equation, the two last terms describe, respectively, the Coriolis and the centrifugal acceleration contributions. We are interested in stationary fluids so we did not include dissipation terms that vanish for these configurations. We consider incompressible fluids (*i.e.*, with vanishing convective derivative,  $d\rho/dt \equiv \partial_t \rho + \mathbf{v} \cdot \bar{\nabla} \rho = 0$ ) and thus the continuity equation reduces to the statement that the velocity is a solenoid vector,  $\bar{\nabla} \cdot \mathbf{v} = 0$ . Note that in the classical Young-Laplace equation,  $\bar{K}$  is the spatial or mean curvature (and not the spacetime curvature).

For a fluid in rigid rotation, the Navier-Stokes equation yields for the pressure:  $P = \frac{1}{2} \rho \Omega^2 r^2 + C$ , where  $C$  is a constant. To make later contact with the relativistic result, we choose to replace the constant quantities  $\{\rho, C\}$  by  $\{\rho_0, k\}$ , with the relation between them being  $C = \rho_0(k - 1)$  and  $\rho = 4\rho_0 k$ . A stationary fluid with a non-axisymmetric boundary profile described by  $f(r, \phi) = r - R(\phi) = 0$  has mean curvature  $\bar{K} = \frac{R^2 + 2R'^2 - RR''}{(R^2 + R'^2)^{3/2}}$ . Introducing the dimensionless quantities

$$\psi = \frac{\phi}{\Omega}, \quad v_o(\psi) = \Omega R(\psi), \quad \tilde{\Omega} = \frac{\sigma \Omega}{\rho_0}, \tag{A.2}$$

the Young-Laplace equation can then be written as

$$\frac{v_o v_o'' - 2v_o'^2 - v_o^2}{(v_o^2 + v_o'^2)^{3/2}} + \frac{1}{\tilde{\Omega}} [(k - 1) + 2k v_o^2] = 0. \tag{A.3}$$

This equation agrees with the NR limit of (3.11), as it should, and gives the equation for the profile of stationary classical lobed configurations. It has the first integral,

$$Q_{\text{NR}} \equiv \frac{v_o^2}{\sqrt{v_o^2 + v_o'^2}} - \frac{1}{2\tilde{\Omega}} [k(1 + v_o^2)^2 - (k + 1)v_o^2], \tag{A.4}$$

obtained by integration of (A.3). By curiosity, note that this is an example of a case where “the limit of an expression is not the expression of the limit” since (A.4) is *not* the NR limit of the first integral (3.12).

## References

- [1] S. Bhattacharyya, V. E. Hubeny, S. Minwalla and M. Rangamani, “Nonlinear Fluid Dynamics from Gravity,” JHEP **0802** (2008) 045 [arXiv:0712.2456 [hep-th]].
- [2] S. Bhattacharyya, V. E. Hubeny, R. Loganayagam, G. Mandal, S. Minwalla, T. Morita, M. Rangamani, and H. S. Reall, “Local Fluid Dynamical Entropy from Gravity,” JHEP **0806**, 055 (2008) [arXiv:0803.2526 [hep-th]].

- [3] P. Kovtun, D. T. Son and A. O. Starinets, “Viscosity in strongly interacting quantum field theories from black hole physics,” *Phys. Rev. Lett.* **94**, 111601 (2005).
- [4] P. Kovtun, D. T. Son and A. O. Starinets, “Holography and hydrodynamics: diffusion on stretched horizons,” *JHEP* **0310**, 064 (2003).
- [5] D. T. Son and A. O. Starinets, “Viscosity, Black Holes, and Quantum Field Theory,” *Ann. Rev. Nucl. Part. Sci.* **57** (2007) 95 [arXiv:0704.0240 [hep-th]].
- [6] R. A. Janik and R. Peschanski, *Asymptotic perfect fluid dynamics as a consequence of ads/cft*, *Phys. Rev.* **D73** (2006) 045013, [hep-th/0512162].
- [7] R. A. Janik and R. Peschanski, *Gauge / gravity duality and thermalization of a boost-invariant perfect fluid*, *Phys. Rev.* **D74** (2006) 046007, [hep-th/0606149].
- [8] S. Bhattacharyya, S. Lahiri, R. Loganayagam, and S. Minwalla, *Large rotating AdS black holes from fluid mechanics*, arXiv:0708.1770 [hep-th].
- [9] M. Van Raamsdonk, *Black Hole Dynamics From Atmospheric Science*, *JHEP* **05** (2008) 106, arXiv:0802.3224 [hep-th].
- [10] M. Haack and A. Yarom, *Nonlinear viscous hydrodynamics in various dimensions using AdS/CFT*, *JHEP* **10** (2008) 063, arXiv:0806.4602 [hep-th].
- [11] M. Haack and A. Yarom, “Universality of second order transport coefficients from the gauge-string duality,” arXiv:0811.1794 [hep-th];
- [12] S. Bhattacharyya, R. Loganayagam, I. Mandal, S. Minwalla, and A. Sharma, *Conformal Nonlinear Fluid Dynamics from Gravity in Arbitrary Dimensions*, *JHEP* **0812**, 116 (2008), arXiv:0809.4272 [hep-th].
- [13] S. Bhattacharyya, R. Loganayagam, S. Minwalla, S. Nampuri, S. P. Trivedi, and S. R. Wadia, *Forced Fluid Dynamics from Gravity*, *JHEP* **0902**, 018 (2009), arXiv:0806.0006 [hep-th].
- [14] J. Erdmenger, M. Haack, M. Kaminski, and A. Yarom, *Fluid dynamics of R-charged black holes*, *JHEP* **0901**, 055 (2009), arXiv:0809.2488 [hep-th].
- [15] N. Banerjee, J. Bhattacharya, S. Bhattacharyya, S. Dutta, R. Loganayagam, and P. Surowka, *Hydrodynamics from charged black branes*, arXiv:0809.2596 [hep-th].
- [16] J. Hur, K. K. Kim, and S.-J. Sin, *Hydrodynamics with conserved current from the gravity dual*, *JHEP* **03** (2009) 036, arXiv:0809.4541 [hep-th].
- [17] M. Torabian and H.-U. Yee, *Holographic nonlinear hydrodynamics from AdS/CFT with multiple/non-Abelian symmetries*, arXiv:0903.4894 [hep-th].
- [18] J. Hansen and P. Kraus, *Nonlinear Magnetohydrodynamics from Gravity*, *JHEP* **04** (2009) 048, [arXiv:0811.3468 [hep-th]].

- [19] M. M. Caldarelli, O. J. C. Dias, and D. Klemm, *Dyonic AdS black holes from magnetohydrodynamics*, JHEP **03** (2009) 025, [[arXiv:0812.0801 \[hep-th\]](#)].
- [20] I. Kanitscheider and K. Skenderis, *Universal hydrodynamics of non-conformal branes*, JHEP **04** (2009) 062, [arXiv:0901.1487 \[hep-th\]](#).
- [21] J. R. David, M. Mahato, and S. R. Wadia, *Hydrodynamics from the D1-brane*, JHEP **04** (2009) 042, [arXiv:0901.2013 \[hep-th\]](#).
- [22] S. Dutta, *Higher Derivative Corrections to Locally Black Brane Metrics*, [arXiv:0804.2453 \[hep-th\]](#).
- [23] M. Rangamani, S. F. Ross, D. T. Son, and E. G. Thompson, *Conformal non-relativistic hydrodynamics from gravity*, JHEP **0901**, 075 (2009), [arXiv:0811.2049 \[hep-th\]](#).
- [24] S. Bhattacharyya, S. Minwalla, and S. R. Wadia, *The Incompressible Non-Relativistic Navier-Stokes Equation from Gravity*, [arXiv:0810.1545 \[hep-th\]](#).
- [25] I. Fouxon and Y. Oz, “Conformal Field Theory as Microscopic Dynamics of Incompressible Euler and Navier-Stokes Equations,” [arXiv:0809.4512 \[hep-th\]](#).
- [26] R. Baier, P. Romatschke, D. T. Son, A. O. Starinets, and M. A. Stephanov, *Relativistic viscous hydrodynamics, conformal invariance, and holography*, JHEP **0804**, 100 (2008), [arXiv:0712.2451 \[hep-th\]](#).
- [27] R. Loganayagam, *Entropy current in conformal hydrodynamics*, JHEP **0805**, 087 (2008), [arXiv:0801.3701 \[hep-th\]](#).
- [28] G. L. Cardoso, G. Dall’Agata and V. Grass, “On Subextensive Corrections to Fluid Dynamics from Gravity,” [arXiv:0906.0587 \[hep-th\]](#).
- [29] P. Figueras, V. E. Hubeny, M. Rangamani and S. F. Ross, “Dynamical black holes and expanding plasmas,” [arXiv:0902.4696 \[hep-th\]](#).
- [30] M. Rangamani, “Gravity & Hydrodynamics: Lectures on the fluid-gravity correspondence,” [arXiv:0905.4352 \[hep-th\]](#).
- [31] O. Aharony, S. Minwalla and T. Wiseman, “Plasma-balls in large N gauge theories and localized black holes,” Class. Quant. Grav. **23**, 2171 (2006) [[arXiv:hep-th/0507219](#)].
- [32] S. Lahiri and S. Minwalla, “Plasmarings as dual black rings,” [arXiv:0705.3404 \[hep-th\]](#).
- [33] E. Witten, “Anti-de Sitter space, thermal phase transition, and confinement in gauge theories,” Adv. Theor. Math. Phys. **2** (1998) 505 [[arXiv:hep-th/9803131](#)];
- [34] D. Mateos, “String Theory and Quantum Chromodynamics,” Class. Quant. Grav. **24** (2007) S713 [[arXiv:0709.1523 \[hep-th\]](#)].

- [35] S. Bhardwaj and J. Bhattacharya, “Thermodynamics of Plasmaballs and Plasmarings in 3+1 Dimensions,” arXiv:0806.1897 [hep-th].
- [36] M. M. Caldarelli, O. J. C. Dias, R. Emparan and D. Klemm, “Black Holes as Lumps of Fluid,” JHEP **0904** (2009) 024 [arXiv:0811.2381 [hep-th]].
- [37] K. i. Maeda and U. Miyamoto, “Black hole-black string phase transitions from hydrodynamics,” arXiv:0811.2305 [hep-th].
- [38] V. Cardoso and O. J. C. Dias, “Bifurcation of Plasma Balls and Black Holes to Lobed Configurations,” JHEP **0904** (2009) 125 [arXiv:0902.3560 [hep-th]].
- [39] J. Bhattacharya and S. Lahiri, “Lumps of plasma in arbitrary dimensions,” arXiv:0903.4734 [hep-th].
- [40] L. M. Hocking, “The stability of a rigidly rotating column of liquid,” *Mathematika* **7**, 1 (1960);  
L. M. Hocking and D. H. Michael, “The stability of a column of rotating liquid,” *Mathematika* **6**, 25 (1959).
- [41] R. E. Benner, O. A. Basaran, L. E. Scriven, “Equilibria, Stability and Bifurcations of Rotating Columns of Fluid Subjected to Planar Disturbances,” *Proc. Math. and Phys. Sciences* **433** (1991) 81.
- [42] O. J. C. Dias, T. Harmark, R. C. Myers and N. A. Obers, “Multi-black hole configurations on the cylinder,” *Phys. Rev. D* **76** (2007) 104025 [arXiv:0706.3645 [hep-th]].
- [43] R. Gregory and R. Laflamme, “Black strings and p-branes are unstable,” *Phys. Rev. Lett.* **70**, 2837 (1993) [arXiv:hep-th/9301052].
- [44] V. Cardoso and O. J. C. Dias, “Gregory-Laflamme and Rayleigh-Plateau instabilities,” *Phys. Rev. Lett.* **96**, 181601 (2006) [arXiv:hep-th/0602017].
- [45] R. Emparan and R. C. Myers, “Instability of ultra-spinning black holes,” JHEP **0309** (2003) 025 [arXiv:hep-th/0308056].
- [46] O. J. C. Dias, P. Figueras, R. Monteiro, J. E. Santos and R. Emparan, “Instability and new phases of higher-dimensional rotating black holes,” arXiv:0907.2248 [hep-th].
- [47] V. Cardoso and L. Gualtieri, “Equilibrium configurations of fluids and their stability in higher dimensions,” *Class. Quant. Grav.* **23** (2006) 7151 [arXiv:hep-th/0610004].
- [48] S. Chandrasekhar, “The stability of a rotating liquid drop,” *Proc. Roy. Soc. Ser. A* **286**, 1 (1965).
- [49] R. A. Brown and L. E. Scriven, “The shape and stability of rotating liquid drops,” *Proc. Roy. Soc. London Ser. A* **371**, 331 (1980).

- [50] R. J. A. Hill and L. Eaves, “Polygonal excitations of spinning and levitating droplets”, arXiv:0808.3704 [physics].